IMPACT OF CONTINUOUS ATMOSPHERIC PRESSURE PLASMA POLYMERISATION OF ACRYLIC ACID ON THE INTERFACIAL PROPTERTIES OF CARBON FIBRE - RFL ELASTOMER COMPOSITES

S. Bai[1], K.K.C. Ho[1], G. Knox[2], A. Bismarck[1*]

[1] *Department of Chemical Engineering, Polymer and Composite Engineering (PaCE) Group, Imperial College London, South Kensington Campus, London SW7 2AZ, UK*
[2] *Power Transmission Division, Gates Corporation, Rochester Hills, U.S.*
* *a.bismarck@imperial.ac.uk*

Keywords: Atmospheric plasma polymerization, Carbon fibre, Resorcinol/ formaldehyde/ latex (RFL), Acrylic acid

Abstract
An atmospheric pressure plasma polymerisation (APP) route to enhance the adhesion properties between carbon fibres and elastomeric matrix was developed. The surface chemistry and physical properties of the modified carbon fibres were characterised to examine the impact of APP treatment on carbon fibres in regards to different treatment times. The wettability of treated carbon fibres was significantly improved as result of the introduction of chemical functionalities to the fibre surface, which was indicated by XPS measurements. Micromechanical characterisation of adhesion behaviour between carbon fibres and elastomeric matrix showed significant improvement by around 60% with the longest treatment time.

1 Introduction

Elastomeric belting is widely used to provide power transmission in automotive and industrial applications. A typical synchronous belt composite consists of three components, namely rubber matrix (body), reinforcement which consists of continuous fibers to provide tensile strength, and an abrasion resistant fabric on the tooth profile of the belt composite. As with many high performance composites, belt performance relies greatly on the quality of the bonding between fibres and elastomers in order to function correctly, as the mechanical properties of the composite depend intrinsically on the interfacial properties [1]. The cord is responsible for carrying the load, contributing to good dynamic behaviour of belts as well as allows for flexibility. In rubber belt system, since rubber compounds exhibit high elongation with relatively low strength, and most man-made fibres, such as aramid and polyester fibres, hardly adhere to elastomeric matrix due to their incompatibility, therefore, a RFL was used as an adhesive bridging the gap between fibres and rubber compounds properties and to protect the cord from interfilament abrasion for the overall best performance. In order to get a compact drive component, which can be integrated with a lot of power in a small confined space and providing versatility to drive designers; a reduced width belt with high power transmission capacity, strength, flexibility and durability, chemical resistance, low elongation, and a wide operational temperature is required. Therefore, carbon fibres, compared to other

reinforcements, with higher specific strength and modulus, better chemical resistance and dimensional stability [2], are ideal used for high performance power transmission belts. However, poor adhesion between carbon fibres and RFL, leading to "belt tensile decay", with the failure mode of delamination of the belt teeth from the cord, is the main problem of the current carbon belt system. Mechanical interlocking is known to be the main interaction between the fibres and the RFL as compared to chemical bonding. Therefore, the primary function of a fibre surface modification is to introduce more functional groups reacting with the RFL to form more chemical bonding and then to create optimum adhesion at the fibre-matrix interphase. APP with a stable and uniform plasma environment at atmospheric pressure allows carbon fibres to be treated uniformly and continuously [3, 4]. In this study, a continuous APP route for modifying the carbon fibres to achieve good adhesion to RFL elastomer and therefore to enhance the load carrying capability and fatigue life of the carbon fibre / elastomer composite was employed.

2Methodology

APP was performed on unsized PAN based carbon fibre in an Openair® plasma Technology system (Plasma Jet PFW10-PAD; Plasmatreat®, Steinhagen, Germany). Air was used as ionization gas. Precursors used for APP was acrylic acid (99 % purity, Aldrich, UK). Different APP treatment configurations (Figure1.) were explored to determine the optimum way to modify carbon fibres continuously in atmospheric plasma. The precursor vapour was supplied with the same dosing rate by nebuliser. The carbon fibre roving was positioned at a distance of 15 mm from the tip of the plasma jet inside a 25 cm long borosilicate glass 3.3 unequal tee piece (PTU100/25, QVF Process System Ltd, Stafford, UK). The configuration shown in Figure1 allows the fibres to be continuously treated with both sides of the carbon fibre roving are exposed to the plasma jet. The carbon fibres were redirected by means of PTFE roller pins allowing the fibres to be looped 3 times through the glass chamber, therefore, maximising the fibres exposure to APP. A stainless steel mesh was/was not placed between the top carbon fibre roving and the second fibre roving. The function of stainless steel was to block part of ionized particles, and then to reduce the physical sputtering of plasma on the rest of fibre roving. Acrylic acid vapour will be polymerised onto fibre surface by UV and rare energetic particles. Without stainless steel, there will be the competition between polymerisation of precursor and physical sputtering of plasma during APP treatment. Five different treatment speeds 0.18, 0.4, 0.8, 1.4, 2.5, 5 m/min were chosen corresponding to residual times within the glass chamber of 4.2 min, 1.9 min and 0.9 min, 0.5min, 0.3min, 0.15min, respectively. In order to examine the influences of APP on carbon fibres and the interfacial interaction between fibre and elastomeric matrix, the surface and bulk properties characterisations of carbon fibres has been conducted, including dynamic contact angle, zeta-potential, BET surface area, XPS, single fibre tensile strength measurements, and micromechanical characterisation of adhesion behaviour of carbon fibre and RFL elastomeric matrix has been characterised through single fibre fragmentation tests on model composites.

3 Results and discussion

3.1 Surface area and *surface morphology of fibres*

It is well known that mechanical interlocking can be a major contribution to the measured practical adhesion. To quantify the influence the surface roughness of the fibres on the adhesion to matrix, the BET surface area A_s of the carbon and glass fibres was determined, as shown in Table 3. The surface areas of APP treated carbon fibres were a bit higher than that of untreated carbon fibres, but an increase to at least 5–10 m^2/g is required to have any

significant effect on practical adhesion. Therefore, the small changes in surface area of the carbon fibre are not expected to make for any mechanical interlocking between the fibres and the matrix [5, 6]. The surface morphologies of carbon fibre examined using the SEM (Figure 2.) showed that after APP treatment there were deposited polymer films on carbon fibre surfaces. After the longest APP treatment time, carbon fibres treated under the configuration with mesh had thicker deposited polymer film than the one of without mesh. With the APP processing speed increase, the smaller polymer chains were formed.

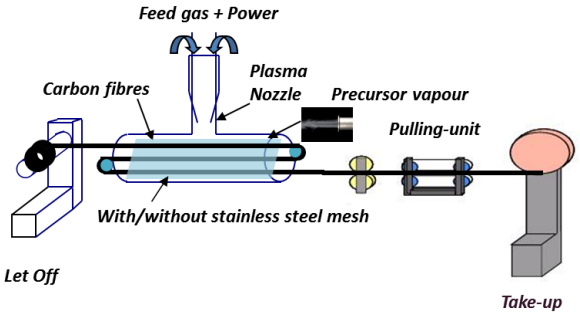

Figure 1. Schematic of continuous atmospheric plasma polymerisation(APP) treatment set-up for carbon fibres.

3.2 Wettability and surface energy of carbon fibres

The contact angles were measured using the modified-Wilhemy method, significant increases in surface hydrophilicity (Table 1) and higher surface energies were observed for APP treated carbon fibres (Table 3). With the reducing APP treatment time, the water contact angles dropped and surface free energy increased further. The increase in the carbon fibre surface energy should lead to better wettability of the fibres by the matrix and, therefore, to a more intimate contact between the phases. The water contact angle hysteresis of APP treated carbon fibres with the longer treatment time, defined as the difference between θ_a and θ_r, was higher than untreated carbon fibres. But the hysteresis of carbon fibres with the processing speed above 1.4m/min was lower than untreated carbon fibres, which indicates the surface of fibres was more chemically homogenous and/or due to the surface roughness decreases.

3.3 XPS surface analysis

The influence of APP treatment on the surface composition of carbon fibres was investigated by XPS (Table 1.). Opposite our expect, under the configuration without mesh, the oxygen and nitrogen content of APP treated carbon fibres were both increased with the APP treatment time decreased. The deconvolution of the high resolution spectra of C 1s on the APP treated carbon fibres (Figure 4A.) showed the shorter residence time in the plasma, the more COOH-groups were introduced and the more CH_x groups were correspondingly dropped. The higher carboxylate content can lead to the higher surface free energy (Figure 4B). Also, the surface carboxylate content follows that of nitrogen, showing that air and acrylic acid were simultaneously incorporated into the surface, but the less time the fibre spends in the plasma, the greater the extent of fibre modification. However, with the longest residence time in plasma, carbon fibres treated under the configuration with mesh had much higher the nitrogen and oxygen content than that APP treated without mesh. The surface compositions and surface free energy of it were similar with that of carbon fibres treated shorter time without mesh. The reason why longer residence time can lead to less carboxylate content for the carbon fibres treated under the configuration without mesh is because chemical etching and physical sputtering were competitive with polymerisation of acrylic acid. The stainless steel

mesh reduced this competition in processing, which was beneficial for more carboxylate introduced.

3.4 ζ –potential analysis

The pH-dependent ζ-potential measurements of carbon fibres (Figure 3) were performed to characterise the acidic/basic characters of the fibres. All the fibres showed a typical behaviour of solid containing acidic groups with the indication of low isoelectric point (i.e.p.), and the ζ-potential plateau in the alkaline region [7, 8] ($6 < pH < 10$). At high pH all acidic functional groups are dissociated. When reducing the pH the dissociation is repressed until the i.e.p. is reached and all acid groups are fully protonated, so the surface carries no charge. With the longest APP treatment time, carbon fibres treated without mesh display a less acidic character with the i.e.p. at pH 3.6. The untreated and carbon fibres treated with mesh had low i.e.p. values which were not experimentally accessible. But the low i.e.p. values can reflect that high acidic surface character and the existing surface groups have a low affinity to protons (Bismarck et al., 2004). The position of i.e.p. is determined by the concentration and relative strength (pKa) of all dissociating surface groups present. With the exposure time to APP decrease, the ζ-potential changes, the surfaces of the fibres were more acidic as compared to the fibres treated with longer time. The i.e.p. for APP treated fibres shifts from pH 3.6 to an extrapolated pH 2.4 and even low i.e.p values. And it can be seen that the ζ-potential plateau value increases with reducing the treatment time, as more dissociable acidic functional groups existed on fibres.

3.5 Adhesion behaviour analysis: single fibre fragmentation test

Single fibre fragmentation tests were performed to determine the adhesion between carbon fibres and RFL. A shorter fragment length can result from an enhanced fibre/matrix adhesion and/or a lower tensile strength of the fibre. Therefore, a quantitative study of the interfacial shear strength was carried out using the Kelly–Tyson model [9] and the Weibull fitting (Figure 5B) to predict the fibre tensile strength at the critical length. Meanwhile, single fibre tensile strength and modulus were not affected by APP treatment as shown in Table 2. The tensile strength of all carbon fibres had a length dependence due to the flaw-induced nature of fibre failure [10, 11], with the average strengths of all the carbon fibres decreased with increasing gauge length. On the contrary, the fibre modulus remained constant as expected with the increasing of gauge length since they were not affected by the flaws along the fibres but dominated by the fibre core structure. The apparent interfacial shear strength (IFSS) of carbon fibres treated with the longest time and no mesh to RFL elastomer significantly increased by around 60% compared to that of untreated carbon fibres (Table 4), and it was also slightly higher than that of the fibres treated for the same length of time but using mesh. The increase of processing speed can lead to the decrease of the apparent IFSS, though there were more functionalities induced and better wettability (Figure 5A). The shorter residence time in plasma might leads to partially polymerized acrylic acid with shorter polymer chains, which can cause the lower mechanical properties of polymerized polymer. Therefore, the weaker interphase formed and had negative effect on the IFSS. With the longest residence time, the carbon fibres treated using mesh had more functionalities than the one treated without mesh, but it had slightly lower IFSS was due to the gradient polymer structure, which might have some structure defects inside. The carbon fibre treated without using mesh might have denser deposited polymer layer with better mechanical property. This together with the higher wettability and functionalites induced by plasma might be the main attribute to the higher IFSS.

4 Conclusions

A newly developed continuous atmospheric pressure plasma polymerisation (APP) route to enhance the adhesion properties between carbon fibres and elastomeric matrix was introduced and the impact of continuous APP on the surface chemisty and mechanical properties of carbon fibres was examined. The effect of residual time of carbon fibres in an APP environment with different configurations was investigated using XPS, wettability measurements, ζ-potential and single fibre fragmentation test. The bulk properties of the continuous APP treated fibres were not affected with lossless of tensile strength and modulus. Micromechanical characterisation of adhesion behaviour between carbon fibres and elastomeric matrix showed significant improvement by around 60% with the longest treatment time. The increased wettability can induce better adhesion, but the mechanical properties of deposited polymer were crucial for IFSS. The shorter resident time in plasma can lead to more carboxylate existing on the fibre surface, but it can also lead to lower mechanical properties of deposited polymers, which resulted in lower IFSS. The using of stainless steel mesh increased the content of carboxylate, also it lead to a different physical structure of deposited polymer layer, which induced a slightly lower IFSS compared to without using mesh.

Fibre investigated	**θa (W) / °**	**θr(W) / °**	**Δθ (W)/ °**	**O 1s / at.%**	**N 1s / at.%**	**C 1s / at.%**
As received	68.7 ± 0.6	60.3 ± 0.3	8.4	11.95	1.48	86.57
0.18m/min-wish mesh	60.6 ± 1.7	50.6 ± 0.5	10.0	13.04	2.64	84.31
0.18m/min-no mesh	49.8 ± 2.1	34.9 ± 1.5	14.9	10.62	0.6	88.78
0.4m/min-no mesh	54.6 ± 0.4	41.4 ± 0.8	13.2	13.08	1.83	85.09
0.8m/min-no mesh	47.1 ± 1.5	34.7 ± 1.6	12.4	12.35	1.95	85.71
1.4m/min-no mesh	42.1 ± 2.1	39.8 ± 1.3	2.3	12.24	3.28	84.48
2.5m/min-no mesh	45.0 ± 1.3	39.3 ± 1.0	5.7	14.18	3.77	82.05
5 m/min-no mesh	46.9 ± 1.5	40.6 ± 0.8	6.3	13.89	4.54	81.57

Table 1. Dynamic water contact angles and surface composition (in at.%) of atmospheric plasma polymerisation treated carbon fibres determined by XPS

	Fibres	**Gauge length / mm * (×25 samples)**		
		20*	**25***	**30***
Tensile Strength / MPa	As received	4066 ± 188	3946 ± 124	3829 ± 136
	0.18m/min-no mesh	4112 ± 186	3773 ± 222	3710 ± 262
Young's Modulus/ GPa	As received	219 ± 2.5	239 ± 4.3	237 ± 5.4
	0.18m/min-no mesh	242 ± 5.0	248 ± 4.7	250 ± 3.1

Table 2. Tensile strength and Young's modulus at different gauge lengths of untreated/ APP modified carbon fibres.

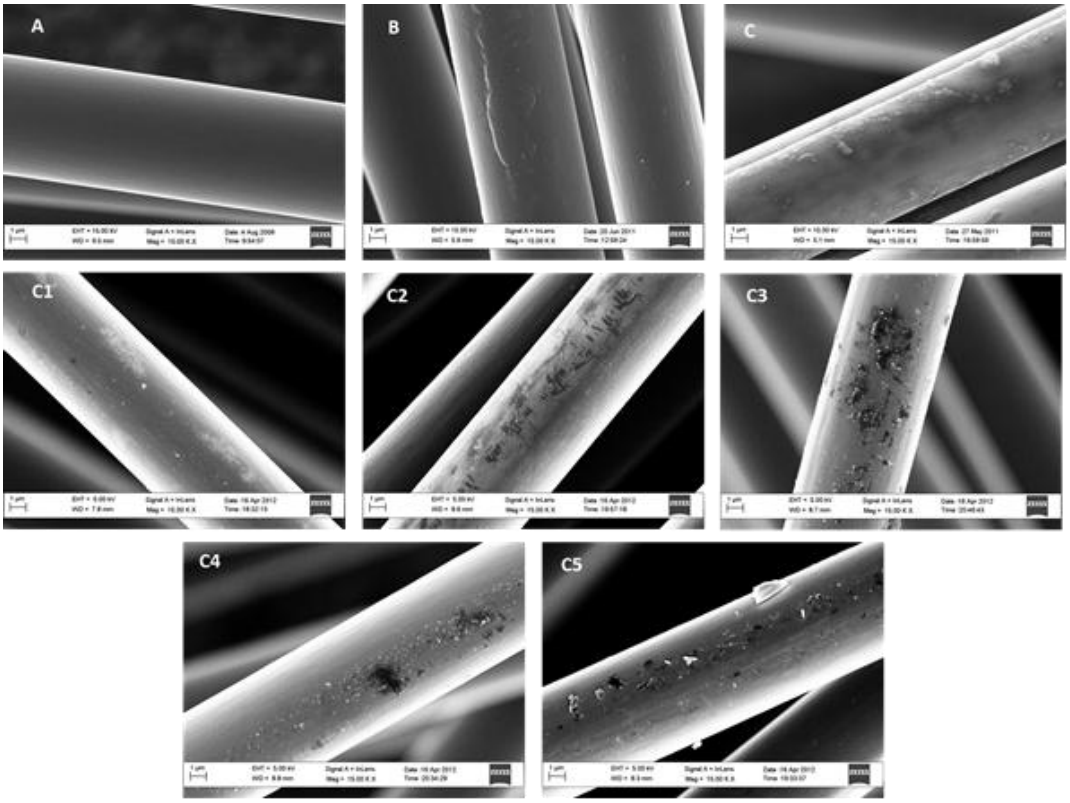

Figure 2. SEM images of APP treated PAN based carbon fibres (A) untreated,(B)0.18m/min-with mesh, (C)0.18m/min-no mesh,(C1)0.4m/min-no mesh,(C2)0.8m/min-no mesh,(C3)1.4m/min-no mesh,(C4) 2.5m/min-no mesh, (C5) 5m/min-no mesh.

Fibers	**γ_s (AB)/ mN/m**	**γ_s^{LW} / mN/m**	**γ_s^{AB} / mN/m**	**γ_s^+/ mN/m**	**γ_s^-/ mN/m**	**Diameter**	**A_S/ (m^2/g)**
As received	40.9 ±1.2	29.9 ±0.4	11.1 ±0.7	7.9 ±0.3	3.9 ±0.4	7.1 ±0.1	0.37
0.18m/min-wish mesh	53.1 ±2.3	42.1 ±0.6	11.1 ±1.7	4.2 ±0.5	7.4 ±1.4	7.1 ±0.1	0.38
0.18m/min-no mesh	56.7 ±2.3	42.4 ±0.6	14.3 ±1.7	3.0 ±0.3	16.8 ±2.3	7.0±0.1	0.37
0.4m/min-no mesh	54.2 ±1.6	44.4 ±0.5	9.8 ±1.1	1.5 ±0.3	16.0 ±0.9	7.5 ±0.1	0.39
0.8m/min-no mesh	56.8 ±2.1	42.5 ±0.7	14.3 ±1.5	2.5 ±0.3	20.3 ±1.8	6.9 ±0.1	0.38
1.4m/min-no mesh	56.1 ±1.9	42.3 ±0.5	13.8 ±1.5	1.7 ±0.2	27.3 ±2.5	7.2 ±0.1	0.38
2.5m/min-no mesh	58.2 ±2.0	45.2 ±0.8	13.0 ±1.2	1.9 ±0.2	22.2 ±1.5	6.8 ±0.1	0.39
5 m/min-no mesh	58.3 ±1.9	46.9 ±0.7	11.4 ±1.3	1.6 ±0.2	20.7 ±1.7	6.8 ±0.1	0.39

Table 3. Fibre diameter, BET surface area and surface free energies calculated using acid-base approach (γs(AB)) and of untreated/ APP treated carbon fibres.

Fibres	m	σ_0/ MPa	σ_f/ MPa	d_f / µm	l / µm	l_c/ µm	τ_{IFSS}/ MPa
As received	5.82	6987	6442	7.1	770 ±14	1027 ±18	22.3 ±0.4
0.18m/min-wish mesh	5.78	7484	7299	6.9	555 ±14.8	740 ±20	33.9 ±0.9
0.18m/min-no mesh	5.78	7484	7363	6.9	528 ±14.2	704 ±19	35.9 ±1.0
0.4m/min-no mesh	5.78	7484	7000	6.9	700 ±16.5	933 ±2 2	25.8 ±0.6
0.8m/min-no mesh	5.78	7484	6747	6.9	858 ±21.3	1144 ±28	20.3 ±0.5
1.4m/min-no mesh	5.78	7484	6747	6.9	858 ±26.6	1144 ±35	20.3 ±0.6

Table 4. Weibull distribution parameters and single fibre fragmentation test results for the carbon fibres determined through single fibre fragmentation tests. The fibre tensile strengths at critical length are predicted from the Weibull distribution.

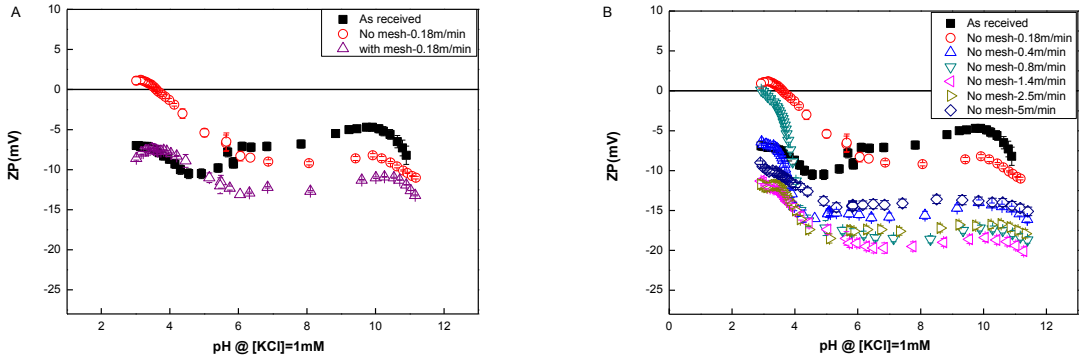

Figure 3. Zeta (ζ) –Potential as function of pH of untreated carbon fibres and of carbon fibres APP treated (A) at speed of 0.18m/min with and without mesh, (B)without mesh at different speeds.

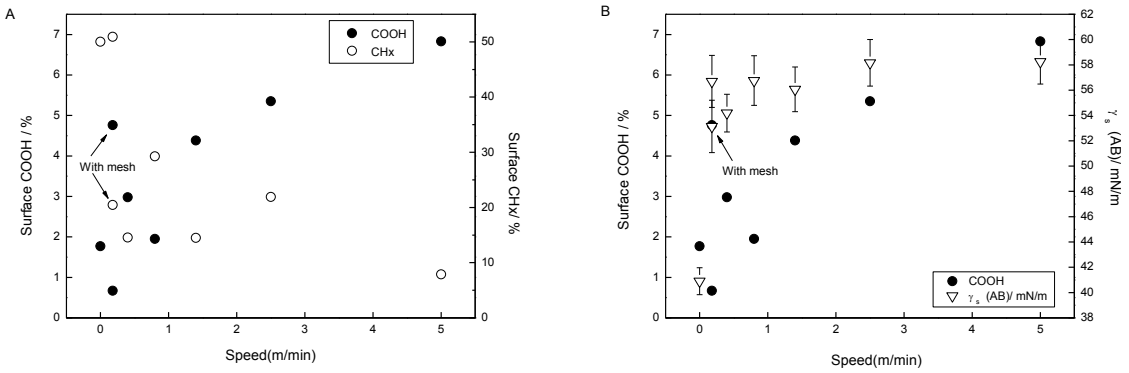

Figure 4. (A) Surface COOH groups and surface CHx groups as functions of APP treatment speed,(B) Surface COOH groups and surface free energy as functions of APP treatment speed.

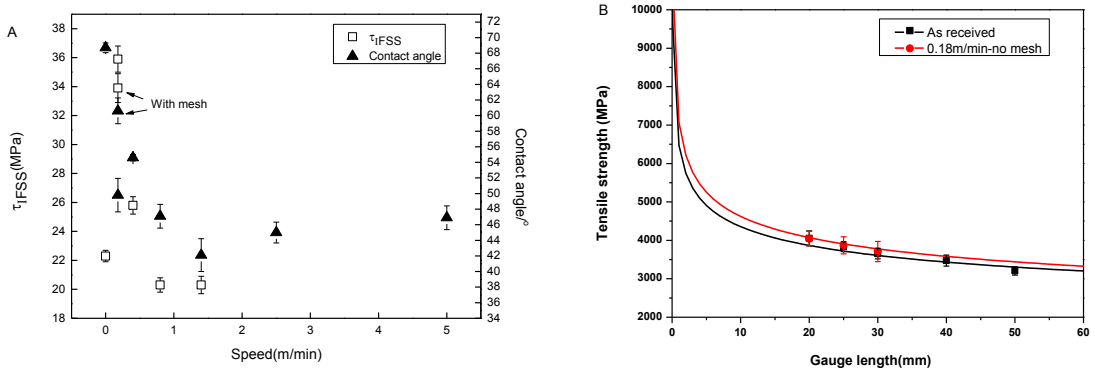

Figure 5. (A)Contact angle and τ_{IFSS} as functions of APP treatment speed. (B)Single fibre tensile strength plotted as a function of gauge length for carbon fibres. The Weibull distribution (shown as lines) was used to account for the gauge length dependence of the tensile strength.

References

[1] J.-K. Kim and Y.-w. Mai, "High strength, high fracture toughness fibre composites with interface control--A review," *Composites Science and Technology*, vol. 41, pp. 333-378, 1991.
[2] J. Donnet, *Carbon fibers*: Marcel Dekker, 1998.
[3] U. Lommatzsch and J. Ihde, "Plasma Polymerization of HMDSO with an Atmospheric Pressure Plasma Jet for Corrosion Protection of Aluminum and Low-Adhesion Surfaces," *Plasma Processes and Polymers*, vol. 6, pp. 642-648, 2009.
[4] M. Jasso, *et al.*, "Coating of PET cords at atmospheric pressure plasma discharge in the presence of butadiene/nitrogen gas mixtures," *Surface and Coatings Technology*, vol. 201, pp. 57-62, 2006.
[5] J. I. Paredes, *et al.*, "Comparative study of the air and oxygen plasma oxidation of highly oriented pyrolytic graphite: a scanning tunneling and atomic force microscopy investigation," *Carbon*, vol. 38, pp. 1183-1197, 2000.
[6] P. Serp, *et al.*, "Surface treatments of vapor-grown carbon fibers produced on a substrate," *Carbon*, vol. 36, pp. 1791-1799, 1998.
[7] I. Aranberri-Askargorta, *et al.*, "Wetting behavior of flax fibers as reinforcement for polypropylene," *Journal of Colloid and Interface Science*, vol. 263, pp. 580-589, 2003.
[8] D. Sharp, *The Penguin dictionary of chemistry*: Penguin Books, 1990.
[9] A. Kelly and W. R. Tyson, "Tensile properties of fibre-reinforced metals: Copper/tungsten and copper/molybdenum," *Journal of the Mechanics and Physics of Solids*, vol. 13, pp. 329-338, in1-in2, 339-350, 1965.
[10] E. G. Stoner, *et al.*, "An end-effect model for the single-filament tensile test," *Journal of Materials Science*, vol. 29, pp. 6561-6574, 1994.
[11] S.-J. Park, *et al.*, "Studies on PAN-based carbon fibers irradiated by Ar+ ion beams," *Journal of Colloid and Interface Science*, vol. 261, pp. 393-398, 2003.